Received: 9 July 2024 | Revised: 18 October 2024 | Accepted: 18 October 2024

DOI: 10.1111/jeu.13066

ORIGINAL ARTICLE

Retention of blue-green cryptophyte organelles by *Mesodinium rubrum* and their effects on photophysiology and growth

Holly V. Moeller[1] | **Amelie L'Etoile-Goga**[1] | **Lucas Vincenzi**[1] | **Andreas Norlin**[1,2] | **Gina S. Barbaglia**[1] | **Gabriel C. Runte**[1] | **Jonatan T. Kaare-Rasmussen**[1] | **Matthew D. Johnson**[3]

[1]Department of Ecology, Evolution, and Marine Biology, University of California, Santa Barbara, Santa Barbara, California, USA

[2]College of Marine Sciences, University of South Florida, St. Petersburg, Florida, USA

[3]Biology Department, Woods Hole Oceanographic Institution, Woods Hole, Massachusetts, USA

Correspondence
Holly V. Moeller, Department of Ecology, Evolution, and Marine Biology, University of California, Santa Barbara, 1120 Noble Hall, Santa Barbara, CA 93106-9620, USA.
Email: hvmoeller@ucsb.edu

Funding information
Simons Foundation, Grant/Award Number: 689265; Division of Molecular and Cellular Biosciences, Grant/Award Number: MCB-2344640 and MCB-2344641; Division of Biological Infrastructure, Grant/Award Number: DBI-1625770; University of California, Santa Barbara, Faculty Senate Research; Health + Life Science Alliance Heidelberg Mannheim

Abstract

As chloroplast-stealing or "kleptoplastidic" lineages become more reliant on stolen machinery, they also tend to become more specialized on the prey from which they acquire this machinery. For example, the ciliate *Mesodinium rubrum* obtains >95% of its carbon from photosynthesis, and specializes on plastids from the *Teleaulax* clade of cryptophytes. However, *M. rubrum* is sometimes observed in nature containing plastids from other cryptophyte species. Here, we report on substantial ingestion of the blue-green cryptophyte *Hemiselmis pacifica* by *M. rubrum*, leading to organelle retention and transient increases in *M. rubrum*'s growth rate. However, microscopy data suggest that *H. pacifica* organelles do not experience the same rearrangement and integration as *Teleaulax amphioxeia*'s. We measured *M. rubrum*'s functional response, quantified the magnitude and duration of growth benefits, and estimated kleptoplastid photosynthetic rates. Our results suggest that a lack of discrimination between *H. pacifica* and the preferred prey *T. amphioxeia* (perhaps due to similarities in cryptophyte size and swimming behavior) may result in *H. pacifica* ingestion Thus, while blue-green cryptophytes may represent a negligible prey source in natural environments, they may help *M. rubrum* survive when *Teleaulax* are unavailable. Furthermore, these results represent a useful tool for manipulating *M. rubrum*'s cell biology and photophysiology.

KEYWORDS
acquired photosynthesis, ciliate, cryptophyte, functional response, *Hemiselmis pacifica*, kleptoplasty

INTRODUCTION

KLEPTOPLASTIDIC – or chloroplast-stealing – lineages give us insight into the physiological challenges that eukaryotic cells face by incorporating photosynthetic machinery into their metabolic repertoire. On one hand, the retention of functional chloroplasts is an energetic boon, allowing for the generation of fixed carbon and energy in the new host cell (Johnson, 2011; Stoecker et al., 2009); in some cases, this acquired metabolism supports rapid population growth (Johnson & Stoecker, 2005; Stoecker et al., 2009) and even bloom formation (Campbell et al., 2010; Herfort, Peterson, Campbell, et al., 2011; Moeller et al., 2016; Montagnes et al., 2008). On the other hand, by capturing light energy, plastids can generate substantial photooxidative stress and thus have the potential to be quite damaging to the kleptoplastidic host cell (Miyagishima, 2023).

Kleptoplastidic lineages employ a variety of strategies to address these physiological challenges (reviewed in Miyagishima, 2023), including upregulating existing damage response machinery (Speijer et al., 2020), limiting retention times and light exposure of plastids (Cartaxana et al., 2018), and evolving repair and regulatory mechanisms for stolen plastids (Hansen et al., 2016; Johnson et al., 2023). In the latter case, regulation may involve the use of laterally transferred genes in the host nucleus (Karnkowska et al., 2023; Wisecaver & Hackett, 2010) or the retention of a prey nucleus (termed a *kleptokaryon*, Johnson et al., 2007) that remains transcriptionally active and directs plastid activity (Hehenberger et al., 2019; Johnson et al., 2007). The kleptokaryon may play an important role in plastid division (Johnson & Stoecker, 2005) and photoacclimation (Johnson et al., 2023), allowing for better regulation and integration of chloroplasts into their new host.

These elaborate, kleptokaryon-involving regulatory mechanisms tend to be found in kleptoplastidic lineages that are also highly specialized on a limited subset of prey (Johnson, 2011; Yamada et al., 2023). For example, the highly photosynthetic ciliate *Mesodinium rubrum* steals chloroplasts, mitochondria, and nuclei from cryptophyte algae in the *Teleaulax*/*Geminigera* clade (Hansen et al., 2013). Although single-cell sequencing of field collections shows the occasional presence of other plastid types, during bloom formation plastids come from a single-prey species (Herfort, Peterson, McCue, et al., 2011; Johnson et al., 2016). Laboratory studies have confirmed that *M. rubrum* can ingest and even grow on non-*Teleaulax* cryptophytes (Hansen et al., 2012; Myung et al., 2011; Park et al., 2007), but none have looked at longer term dynamics and the fate and function of these ingested cryptophytes. While *M. rubrum* can apparently distinguish between some cryptophyte algae during ingestion, and selectively ingests preferred prey types (Jiang & Johnson, 2021; Peltomaa & Johnson, 2017), it may not always do so efficiently. In contrast, *M. rubrum*'s sister species, *M. chamaeleon*, which gets about half of its carbon from photosynthesis (Moeller et al., 2021; Moestrup et al., 2012) (compared to *M. rubrum*'s >95%, Smith & Hansen, 2007), can retain functional plastids from at least half a dozen different cryptophyte algae and support sustained positive growth (Kim et al., 2019; Moeller & Johnson, 2018; Moestrup et al., 2012).

However, when preferred prey are not available, it is unclear how *M. rubrum* populations sustain themselves given the gradual loss of stolen organelles (Johnson et al., 2006), or what the dynamics of plastid replacement with nonpreferred prey might look like. Some studies suggest that *M. rubrum* may transiently rely on bacterivory as a heterotrophic source of carbon (Myung et al., 2006). And the presence of alternate prey types in field sequencing data may be evidence of opportunistic – rather than erroneous – predation (Johnson et al., 2016, 2018). However, it is less clear whether alternative prey plastids are integrated into *M. rubrum*'s metabolism.

Here, we report on ingestion of a blue-green cryptophyte, *Hemiselmis pacifica*, by *M. rubrum*. Based on field observations (Herfort, Peterson, McCue, et al., 2011; Johnson et al., 2016) and past experimental work (Hansen et al., 2012; Myung et al., 2011; Park et al., 2007; Peltomaa & Johnson, 2017), we hypothesized that (1) ingestion of *H. pacifica* would be minimal and would not increase *M. rubrum* growth rates, (2) *M. rubrum* would exhibit a preference for ingesting its preferred prey, *Teleaulax amphioxeia*, over *H. pacifica*, and (3) we would find no evidence of sustained photosynthetic activity or growth benefits from *H. pacifica* plastids. However, the robust capacity for growth and photosynthesis by *M. rubrum*-fed *H. pacifica* (at least for the first 2 weeks of feeding on this alternative prey) surprised us. Although photosynthetic function is reduced and organelle integration is limited, we find evidence that alternate cryptophyte prey may help *M. rubrum* persist during intervals when preferred prey are unavailable. We detail these findings as evidence of experimental capacity to alter organelle retention even in the highly photosynthetic, highly specialized *M. rubrum*.

MATERIALS AND METHODS

Cultures and maintenance

We assessed the performance of *M. rubrum* strain CBJR05 offered the blue-green cryptophyte alga *H. pacifica* CCMP 706 (ordered from the National Center for Marine Algae and Microbiota [NCMA], Bigelow, ME, USA). To maintain *M. rubrum* and to contrast performance of the ciliate when offered its preferred cryptophyte prey, we fed the ciliate the red cryptophyte *T. amphioxeia* (GCEP01) at a ratio of approximately 3 cryptophytes to 1 *M. rubrum* during weekly transfers. All three species were maintained at 18°C in GF/F filtered, autoclaved coastal seawater from Santa Barbara, CA, USA, amended with f/2-Si nutrients (Guillard & Ryther, 1962), with a 12 h light:12 h dark cycle at an illumination of 20 μmol quanta/m^2/s during daylight.

Grazing functional responses and prey selectivity

To quantify the ingestion of *H. pacifica* by *M. rubrum*, we conducted two experiments, one (Experiment 1) with a gradient of *H. pacifica* densities to measure the ciliate's functional response, and a second (Experiment 2) in which we offered *M. rubrum* a mixture of *H. pacifica* and *T. amphioxeia* to test for preferential feeding on the red cryptophyte.

For Experiment 1, we inoculated 25 mL suspension culture flasks with *M. rubrum* at a concentration of 500 cells/mL. We added *H. pacifica* at concentrations of either 1000, 2000, 4000, 4500, 6500, and 11,000 cells/mL,

producing cryptophyte to *M. rubrum* ratios of 2, 4, 8, 9, 13, and 22 *H. pacifica* cells per 1 *M. rubrum* cell. We also inoculated *H. pacifica* into *M. rubrum*-free flasks, to serve as predator-free controls that allowed us to measure growth in the absence of grazing. All experimental treatments were run in triplicate. Each day for 4 days, we fixed a 1-mL sample of each experimental flask in 1% acid Lugol's solution; *M. rubrum* and *H. pacifica* cells were then counted on a compound microscope at 100X magnification (10X objective × 10X ocular) to determine population densities over time. We estimated the growth rates of *M. rubrum* and *H. pacifica* as the slope of a line fit through the log of population size over time.

Following the methods of Jeong and Latz (1994), we used the difference in growth rates between predator-free and predator-present experimental flasks to calculate ciliate ingestion rates. We fit a Holling Type II (saturating) predator functional response (Holling, 1959) to ingestion rates as a function of prey density in order to estimate the clearance rate (a.k.a. attack rate) a and handling time h of *M. rubrum* feeding on *H. pacifica*:

$$\text{Ingestion} = \frac{a \times [H.\ pacifica]}{1 + a \times h \times [H.\ pacifica]}.$$

We also fit a Monod-form (Monod, 1949) saturating function to *M. rubrum*'s growth rate as a function of *H. pacifica* density to assess the sensitivity of the ciliate's growth to prey availability:

$$\text{Growth} = \frac{g_{\max} \times [H.\ pacifica]}{H + [H.\ pacifica]} + g_0.$$

Here, g_0 is the baseline growth rate of *M. rubrum* in the absence of prey, $g_{\max}$ is the maximum possible increase in that growth rate, and H is the concentration of *H. pacifica* cells that results in half of the maximum increase in growth (i.e. the half-saturation concentration). We also fit linear models to the relationships between ingestion and *H. pacifica* abundance, and growth and *H. pacifica* abundance. We used the Akaike information criterion (AIC) to determine whether linear or saturating models best fit the data. All calculations (and those described next, unless otherwise specified) were performed in R (version 4.3.0, R Core Team, 2023).

For Experiment 2, we inoculated six 25 mL flasks with a mixture of *T. amphioxeia* and *H. pacifica*. Although our intended target concentrations were 5000 cells/mL per species, differences in inoculation efficiency resulted in initial densities of approximately 5000 *T. amphioxeia* cells/mL and 2500 *H. pacifica* cells/mL. To three of these flasks, we added *M. rubrum* at a concentration of approximately 1000 cells/mL, creating two treatments, each run in triplicate. We sampled all flasks daily for 4 days to determine population sizes.

In order to differentiate between *T. amphioxeia* and *H. pacifica* cryptophytes, we used a FlowCam 8400 imaging flow cytometer with a 532-nm laser (Yokogawa Fluid Imaging Technologies, Scarborough, ME, USA). Ciliates and cryptophytes can be differentiated based on particle size and appearance (using the FlowCam's automated image classification system), and the instrument's laser allows us to differentiate between phycoerythrin (PE)-containing (i.e. *T. amphioxeia*) and PE-absent (i.e. *H. pacifica*) particle types. We counted cryptophytes and *M. rubrum* on the FlowCam by diluting experimental samples to a concentration of <2000 cells/mL, and then imaging all particles in 1 mL of the diluted sample. We then classified *M. rubrum* and cryptophytes using image analysis. We used the *flowPeaks* package in R (Ge & Sealfon, 2012) to assign cryptophytes to species based on PE fluorescence. Following determination of population dynamics of all three species, we used the algorithm of Jeong and Latz (1994) to compute species-specific ingestion and clearance rates. We used t tests to test for prey preference as significant differences in *M. rubrum* clearance rates of the two cryptophyte species.

Confirmation of plastid ingestion

We used confocal fluorescence microscopy of fixed *M. rubrum* cells to confirm that *H. pacifica* cells were ingested by *M. rubrum*. We fixed cells in 1% glutaraldehyde and stored them overnight at 4°C to ensure fixation. Within 72 h of glutaraldehyde fixation, we stained DNA by incubating fixed cells for 30 min at room temperature in a 10 μg/mL DAPI solution. After staining, cells were filtered onto a 1-μm pore size polycarbonate white Whatman Nuclepore Track-Etch membrane filter (Whatman, Inc., Florham Park, NJ, USA) and washed 3× with sterile seawater to eliminate background stain fluorescence. Filters were mounted onto glass slides using Type F immersion oil (Olympus Corporation, Tokyo, Japan) and stored frozen until confocal analysis.

We examined samples using a point-scanning confocal microscope (Leica SP8 Resonant Scanning Confocal) with a 63X/1.4 lens. We identified plastids based on the presence of phycobiliproteins: PE (*T. amphioxiea* plastids) and phycocyanin (PC) (*H. pacifica* plastids) absorb and emit different wavelengths of light. Therefore, we measured fluorescence of DAPI (excitation laser = 405 nm, filter range = 412–484 nm), glutaraldehyde (excitation laser = 488 nm, filter range = 501–555 nm), PE (excitation laser = 570 nm, filter range = 570–609 nm), and PC (excitation laser = 620 nm, filter range = 640–660 nm). This allowed us to visualize ciliate nuclei, plastids, and cryptophyte nuclei within individual cells. We collected high-resolution Z-stacks of representative cells at a 0.5-μm slice depth and a 1024 × 1024 pixel resolution. To visualize plastid content, we created maximum intensity projections in all four channels, scaling brightness and contrast for each channel independently, using

Fiji (Schindelin et al., 2012). Overlay images, as well as single-channel grayscale images, are shown.

Long-term feeding impacts on photosynthesis and growth

To determine the capacity of *M. rubrum* for sustained growth on *H. pacifica*, we conducted a 3-week-long experiment (Experiment 3) in which we contrasted the pigmentation, photosynthetic capacity, and growth of *M. rubrum* populations that were either starved or offered *H. pacifica* (three replicates per treatment = six experimental flasks total). To ensure that *H. pacifica* availability was not growth limiting, we allowed *M. rubrum* to feed "ad libitum" by replenishing *H. pacifica* populations to at least 5000 cells/mL whenever populations fell below 1000 cells/mL in the fed treatment. We measured the population sizes of *M. rubrum* and *H. pacifica* daily by counting Lugol's acid-fixed samples on a compound microscope (as in Experiment 1).

Daily for the first four time points, and every 2–3 days thereafter, we collected additional data on *M. rubrum* cells. To examine plastid replacement dynamics, we imaged cells on the FlowCam, and used chlorophyll and PE fluorescence to estimate the cell volume occupied by PE-containing remnant *T. amphioxeia* plastids and PC-containing new *H. pacifica* plastids (see *Calibration of FlowCam measurements* section, next). On the same dates, we measured photosynthetic capacity using a fluorescence induction relaxation (FIRe) system (custom built by M. Gorbunov, Rutgers University, New Brunswick, NJ, USA). In brief, this system measures autofluorescence in response to pulses of photosynthetically active radiation of known intensity to quantify electron transport rates as a function of light availability (Gorbunov & Falkowski, 2004). These fluorescence-based photosynthesis–irradiance curves allowed us to determine dark-acclimated photosynthetic efficiency (F_V/F_M), photosynthetic rates at growth irradiance (P_I), and maximum photosynthetic rates (P_{max}) as described in our previous work (Lepori-Bui et al., 2022; Moeller et al., 2021; Paight et al., 2023). We also measured chlorophyll content directly by filtering a known number of *M. rubrum* cells onto a GF/F filter (Whatman) and extracting pigments overnight in a 90% acetone solution at −20°C. The following day, we quantified chlorophyll concentration using a Trilogy Fluorometer with a 460 nm LED (Turner Designs, San Jose, CA, USA). To avoid contamination of photophysiology measurements by free-living *H. pacifica* cells, we washed subsamples of experimental cultures free of prey using an 8.0-μm polycarbonate transmembrane filter, as described previously (Moeller et al., 2021; Moeller & Johnson, 2018; Peltomaa & Johnson, 2017) before measuring photosynthesis–irradiance curves or filtering for chlorophyll extraction.

Because of the length of our experiment and growth rate of *M. rubrum*, we performed one dilution on Day 8 to prevent *M. rubrum* populations from becoming density limited (e.g. approaching carrying capacity due to nutrient limitation). We performed a fivefold dilution for the fed treatment and a threefold dilution for the starved treatment, commensurate with growth rates and population sizes. We corrected for this dilution (and dilution due to the addition of fresh prey in the fed treatment) by scaling population sizes proportionally to the volumes added. This allowed us to calculate *M. rubrum* growth rates over a sliding 7-day window as the slope of the relationship between the natural log of population size and experimental day.

Calibration of FlowCam measurements

We used the FlowCam to collect data on cell pigmentation. Specifically, we used peak red fluorescence (a proxy for chlorophyll content) and peak yellow fluorescence (a proxy for PE content) to estimate the amount of photosynthetic pigment contained in cells.

To calibrate our FlowCam fluorescence measurements to the amount of cell volume occupied by plastids, we performed a calibration experiment (Experiment 4) in which we simultaneously measured the fluorescence properties of *M. rubrum* cells using the FlowCam and the confocal microscope. During this 19-day experiment, we grew *M. rubrum* cells under three conditions to generate a range of plastid contents: For the first 2 weeks of the experiment, we used two treatments – starved and well fed with *H. pacifica* – to produce populations of cells that, over time, had diminishing numbers of PE plastids and increasing numbers of PC plastids, respectively. On day 15, we split the *H. pacifica*-fed populations into two new treatments: starved and well fed with *T. amphioxeia*. The latter treatment was used to regenerate cells with a mixture of two plastid types.

At eight time points during this experiment (days 1, 3, 6, 9, 12, 15, 17, and 19), we collected FlowCam optical data as described earlier and prepared a 1-mL subsample of cells with glutaraldehyde fixation and DAPI staining for confocal microscopy, also as described earlier. Using the confocal microscope, we collected data on 15 cells per replicate (0.5 μm slice thickness, 256 × 256 pixel resolution); because the experiment was run in triplicate, this represents 45 cells per treatment per experimental time point. After collecting data from three of the four channels described earlier (representing DAPI, PE, and PC), we used a custom Python script (see https://doi.org/10.5281/zenodo.14201363 for all data and scripts used in this manuscript) to compute the percentage of cellular volume occupied by PE or PC plastids. We used nonlinear regression (function *nls* in R) to estimate best-fitting relationships between chlorophyll proxies (FlowCam red fluorescence and confocal total plastid volume) and PE

proxies (FlowCam yellow fluorescence and confocal PE plastid volume) (Figure S1), and developed a statistical model that allowed us to predict PE and PC plastid content with a high degree of accuracy (R^2=0.913 and 0.953, respectively; Figure S2).

RESULTS

Ingestion of *H. pacifica* by *M. rubrum*

We found that ingestion of *H. pacifica* and growth of *M. rubrum* increased as a function of *H. pacifica* population size (Figure 1), indicating that consumption of *H. pacifica* supports at least transient increases in *M. rubrum* growth rates. Ingestion was a saturating function of *H. pacifica* abundance, with a clearance rate (a.k.a. attack rate) a of 7.068×10^{-3} mL per *M. rubrum* per day and a handling time h of 3.331×10^{-2} days (Figure 1A), though we note that a linear functional response was nearly as statistically strong (Figure S3).

Growth was also a saturating function of *H. pacifica* abundance, with a baseline growth rate (in the absence of prey) g_0 of 3.127×10^{-2} per day, a maximum increase in growth g_{max} of 0.4501 per day (leading to a predicted maximum growth rate of 0.4814 per day), and a half-saturation prey abundance H of 15,880 cells per mL (Figure 1B; a linear model gave a worse statistical fit, Figure S3).

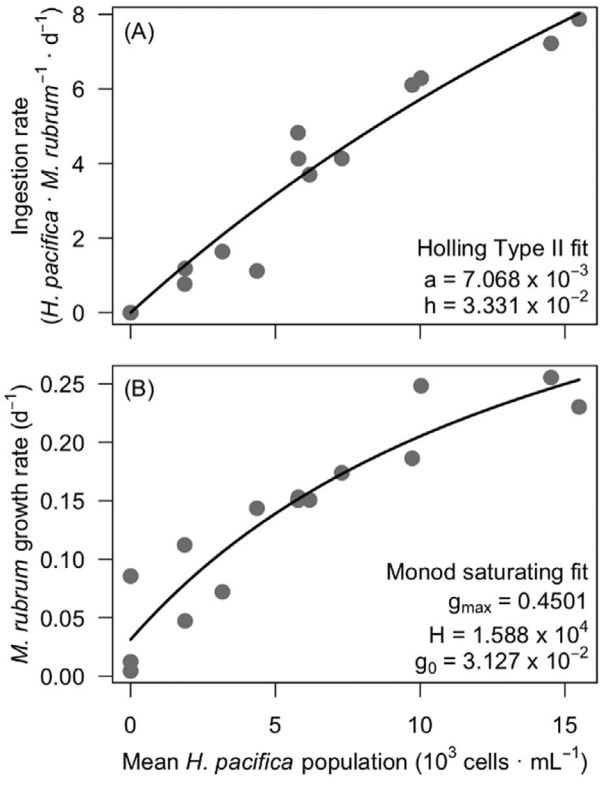

FIGURE 1 *Mesodinium rubrum* ingestion functional response (A) and growth functional response (B) to increasing concentrations of *Hemiselmis pacifica* prey. Both ingestion and growth saturate as prey abundance increases.

We found no evidence of selective grazing by *M. rubrum* when the ciliates were simultaneously offered *T. amphioxeia* and *H. pacifica* (Figure 2). Over time, the population sizes of both cryptophytes declined in the presence of *M. rubrum* (Figure 2A), providing evidence of predation. The growth rate of *H. pacifica* was slightly (but nonsignificantly) lower than that of *T. amphioxeia*, leading to an overall decrease in the relative abundance of *H. pacifica* in the mixed cryptophyte population over time (Figure 2B). However, this decrease was identical to the one observed in the presence of *M. rubrum*, indicating that the two cryptophytes were consumed in proportion to their abundance. Indeed, after controlling for differences in cryptophyte growth rates (Figure 2C) and population sizes (Figure 2D), while the overall ingestion of *T. amphioxiea* was higher (Figure 2E), the clearance rates (a.k.a. attack rates, which represent the "effort" that *M. rubrum* is putting into finding and capturing each cryptophyte species) were statistically identical (Figure 2F, *t*-test p=0.9292).

Photosynthetically active *H. pacifica* plastids are retained by *M. rubrum*

Both compound and confocal fluorescence microscopy confirmed the presence of PC-containing *H. pacifica* plastids inside of *M. rubrum* cells (Figure 3). Furthermore, we observed colocalization of small DAPI-stained puncta (presumably *H. pacifica* nuclei) with *H. pacifica* plastids.

When *M. rubrum* were fed *H. pacifica* over long timescales (Experiment 3), we observed changes in FlowCam measurements of cell fluorescence consistent with ingestion and retention of *H. pacifica* plastids. Specifically, while starved *M. rubrum* showed gradual decreases in both chlorophyll and PE fluorescence, *H. pacifica*-fed *M. rubrum* exhibited sharp decreases in PE fluorescence after 5 days of feeding, though chlorophyll fluorescence was maintained (Figure S4). Based on our calibration between confocal and FlowCam data (Figures S1 and S2), we estimate that these changes in fluorescence correspond to a replacement of PE-containing *T. amphioxeia* plastids (Figure 4A) by PC-containing *H. pacifica* plastids in the fed treatment (Figure 4B), and an overall decline in plastid volume in *H. pacifica*-fed *M. rubrum* (Figure 4C).

Changes in chlorophyll content mirrored this shift in plastids, with *H. pacifica*-fed *M. rubrum* populations showing sharper decreases in per-cell chlorophyll content than starved populations in the last two weeks of the experiment (Figure 5A). However, photosynthetic efficiency of this chlorophyll was higher in fed cells (Figure 5B), though per-chlorophyll photosynthetic rates were lower in *H. pacifica* kleptoplastids (Figure 5C). Within about

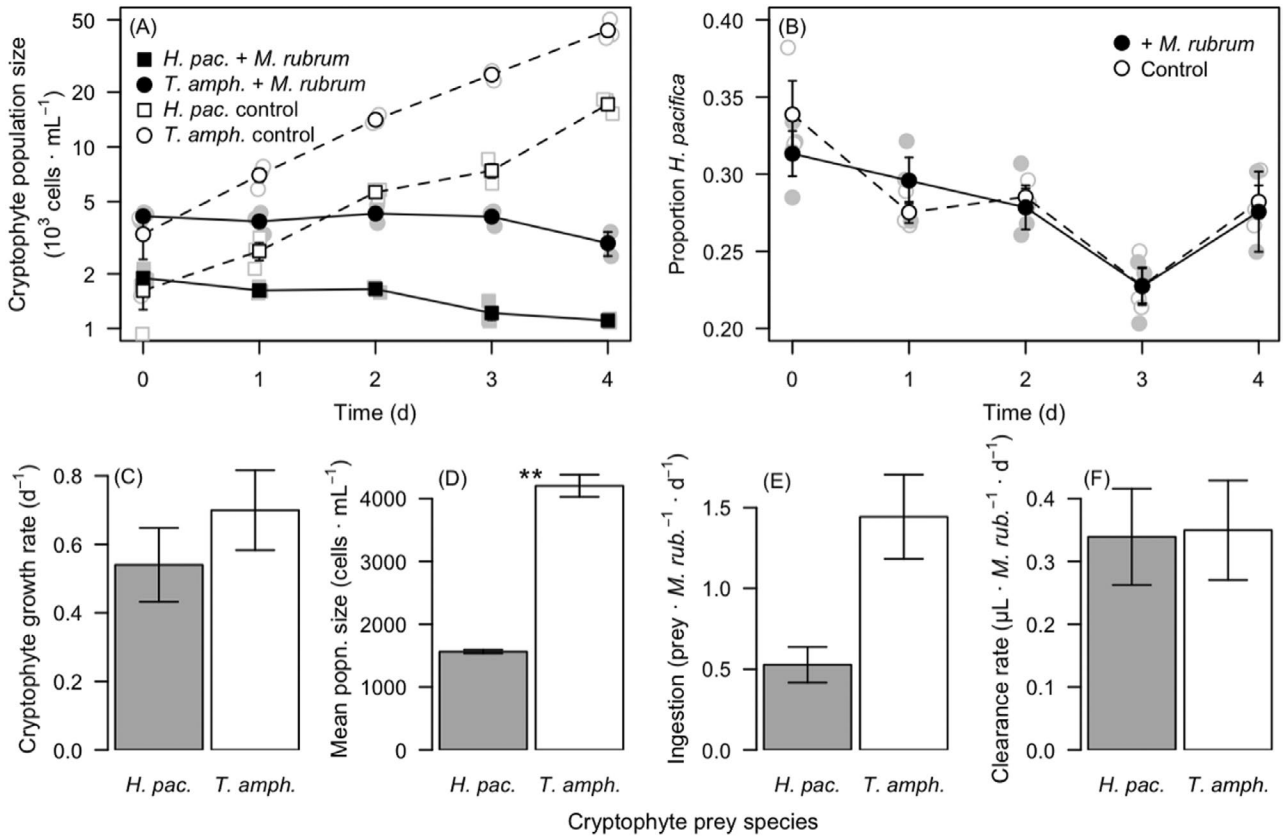

FIGURE 2 No evidence of selective grazing by *Mesodinium rubrum* offered *Hemiselmis pacifica* and *Teleaulax amphioxeia*. (A) Population dynamics of *H. pacifica* and *T. amphioxeia* in the presence (filled symbols) and absence (open symbols) of *M. rubrum*. Lower (negative) growth rates in the presence of *M. rubrum* provide evidence of grazing on both cryptophytes by the ciliate. (B) During the experiment, the relative abundance of *H. pacifica* (which was initially inoculated slightly below the 50:50 intended ratio) did not differ in the two experimental treatments. Because the growth rates of the two cryptophytes were similar (though *H. pacifica* grew nonsignificantly slower, C), the initial difference in population size led to a difference in abundances that persisted throughout the experiment (D). As a result of these numerical differences in prey abundance, ingestion rates of *T. amphioxeia* were higher (E), but the attack rates were identical (F).

2 weeks (the time required for near-elimination of *T. amphioxeia* plastids, Figure 4), *H. pacifica*-fed *M. rubrum* photophysiology came to resemble the photophysiology of free-living *H. pacifica* cells (Figure S5), with faster reductions in maximum photosynthetic rate P_{max}, light sensitivity a, and saturating light intensity E_k than starved *M. rubrum* cells (Figure 5D–F).

Feeding on *H. pacifica* supports transient increases in *M. rubrum* growth rates

Over the course of the 3-week long-term experiment (Experiment 3), we observed increased growth rates in *H. pacifica*-fed *M. rubrum* populations for the first 12 days (Figure 6). This led to an approximate threefold increase in maximum ciliate population size compared to starved cells (Figure 6A). However, after 2 weeks, growth rates in *H. pacifica*-fed and starved cultures were comparable, and growth rates fell below zero (indicating population declines) for both treatments during the third week of the experiment (Figure 6B). Over the course of the experiment, *M. rubrum*-fed *H. pacifica* were generally slightly larger than starved cells, and showed a 25% increase in cell volume after population size plateaued on day 15 (Figure S6).

In the separate experiment designed to calibrate plastid content between the FlowCam and confocal microscope (Experiment 4), we observed that returning *H. pacifica*-fed *M. rubrum* to *T. amphioxeia* prey resulted in replacement of *H. pacifica* plastids with *T. amphioxeia* ones (Figure 2 and Figure S7). This replacement occurred rapidly: within 48 h, two thirds of *H. pacifica* plastids had been eliminated (compared to about one fifth in starved cells; Figure S7). Within 4 days, *M. rubrum* cells had recovered a near-complete complement of *T. amphioxeia* plastids. Even accounting for positive *M. rubrum* growth rates in *T. amphioxeia*-fed cultures, *H. pacifica* plastid volume was lost three times as rapidly in *T. amphioxeia*-fed cultures as in starved cultures (Figure S8).

DISCUSSION

The kleptoplastidic ciliate *M. rubrum* has long been described as a prey specialist, with each described lineage

Eukaryotic Microbiology ISOP Published by the International Society of Protistologists

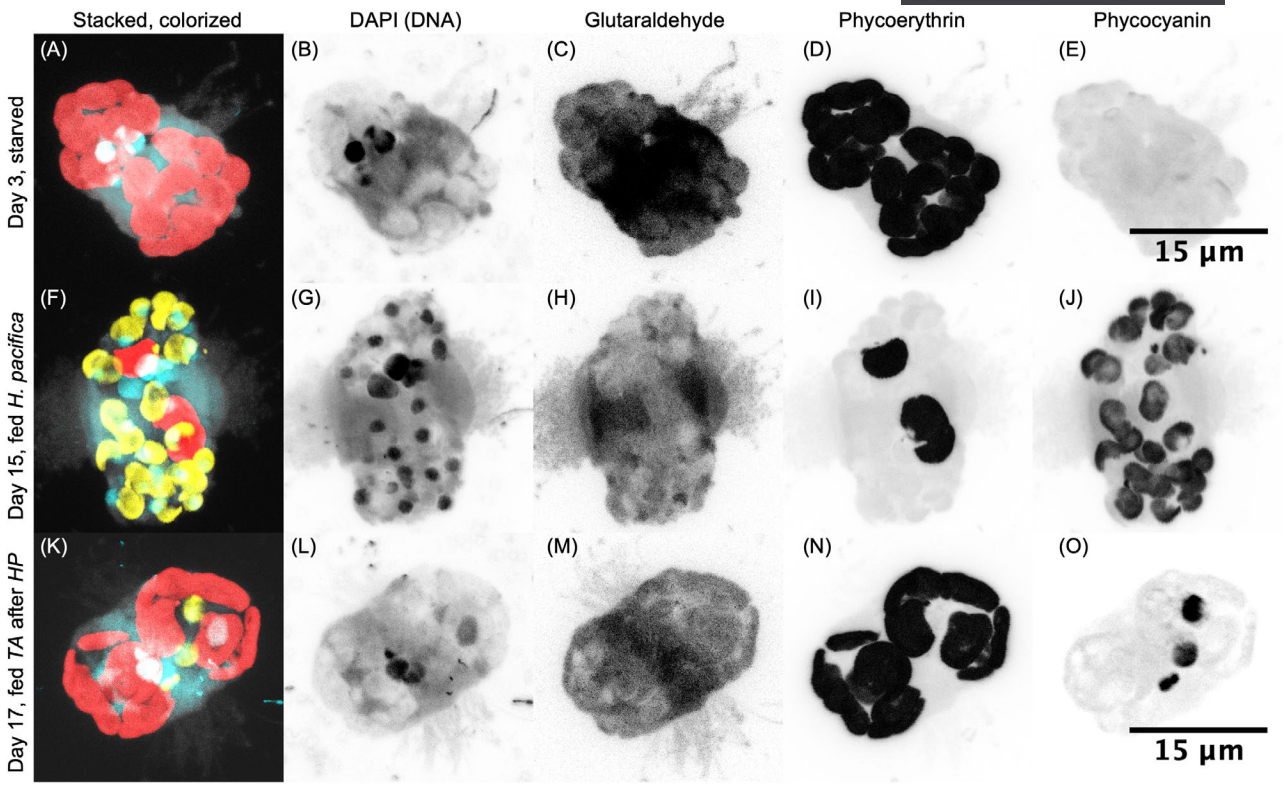

FIGURE 3 Confocal images of *Mesodinium rubrum* subject to different feeding treatments. (A–E) *Mesodinium rubrum*-fed *Teleaulax amphioxeia* and then subject to 3 days of starvation still have numerous phycoerythrin-bearing red plastids. (F–J) After 2 weeks of feeding on *Hemiselmis pacifica*, *M. rubrum* cells are filled with phycocyanin-bearing blue-green plastids; *H. pacifica* nuclei colocalize with these plastids. Typically, one or two *T. amphioxeia* plastids remain. (K–O) After only 2 days of feeding with *T. amphioxeia*, however, *M. rubrum* cells quickly eliminate most *H. pacifica* plastids and re-equip themselves with *T. amphioxeia* plastids.

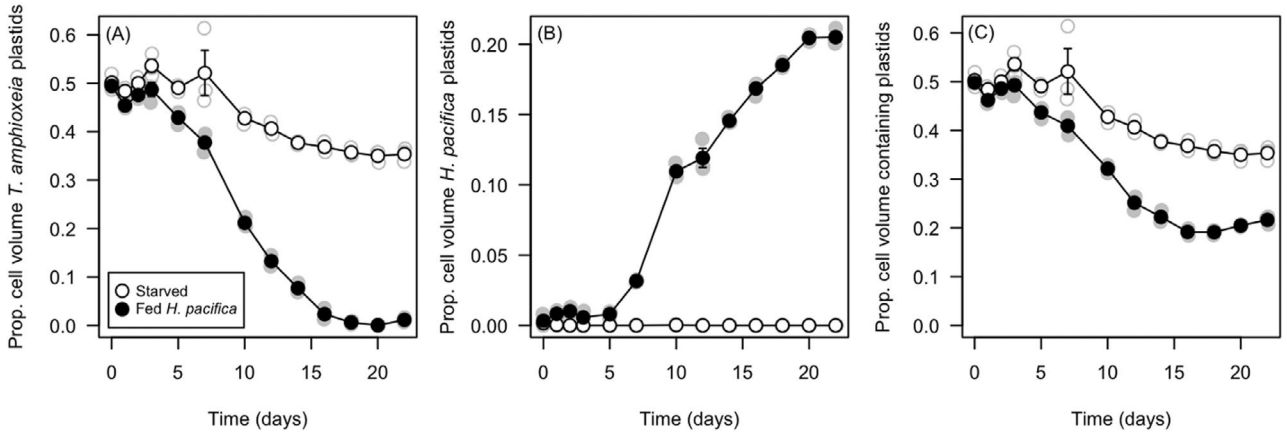

FIGURE 4 Changes in *Mesodinium rubrum* cell volume occupied by (A) *Teleaulax amphioxeia* plastids, (B) *Hemiselmis pacifica* plastids, and (C) all plastid types varied by treatment. While starved cells gradually lost plastid volume over time, *H. pacifica*-fed cells rapidly replaced *T. amphioxeia* plastids after day 5, though the total cell volume occupied by plastids was lower in the *H. pacifica*-fed cultures.

obtaining matched sets of chloroplasts, mitochondria, and transcriptionally active nuclei from specific cryptophyte species in the *Teleaulax*/*Geminigera* clade (Hansen et al., 2013; Johnson et al., 2016). Although in our study, *M. rubrum* could not sustain growth on an alternate prey source indefinitely, we were surprised to observe robust ingestion of the cryptophyte *H. pacifica*, including a lack of discrimination by the ciliate between *H. pacifica* and its optimal prey *T. amphioxeia*, and the presence of photosynthetically active blue-green *H. pacifica* plastids in *M. rubrum*'s cytoplasm. Although we did not track carbon fixed by ingested *H. pacifica* plastids, elevated *M. rubrum* growth rates in fed cultures (even as cell volume remained constant or increased) suggest substantive

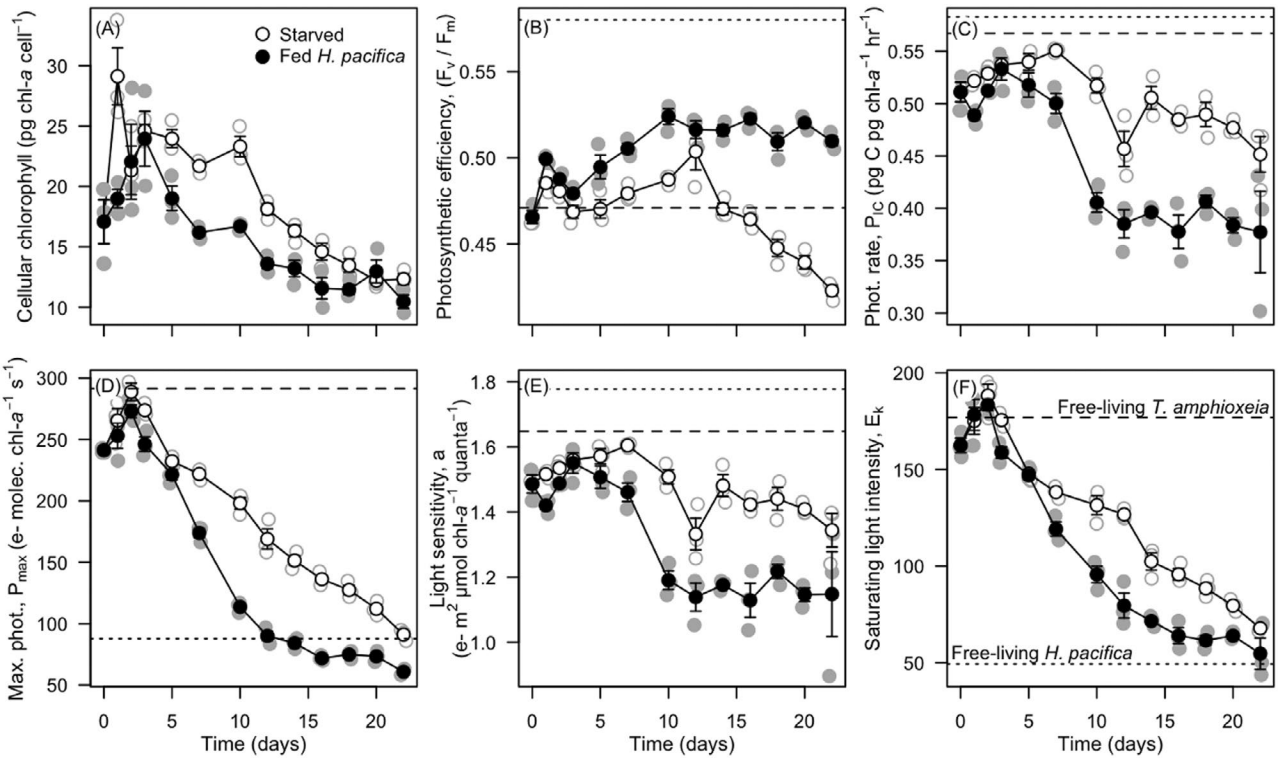

FIGURE 5 Photophysiology of *Mesodinium rubrum* starved (open points) or fed *Hemiselmis pacifica* (filled points). (A) Cellular chlorophyll content decreased in both treatments, but (B) photosynthetic efficiency remained higher for *H. pacifica*-fed cultures. Overall, photosynthesis rates at growth irradiance (C), maximum photosynthetic rates (D), light sensitivity (E), and saturating light intensity (F) were lower for *H. pacifica*-fed cultures. Where applicable, reference lines representing parameters from *Teleaulax amphioxiea* (dashed line) and *H. pacifica* (dotted line) photosynthesis–irradiance curves are shown. Note that *H. pacifica*-fed *M. rubrum* cells still retain some *T. amphioxeia* plastids, which contribute to measurements, especially prior to day 14 (Figure 4).

contributions to carbon and energy acquisition. Our results suggest that nonpreferred plastids observed in *M. rubrum* cells (Johnson et al., 2016) may be photosynthetically active and help sustain *M. rubrum* populations when preferred prey are absent or only available in low abundances.

However, by displacing *T. amphioxeia* plastids during ingestion of *H. pacifica*, *M. rubrum* cells appear to exchange short-term growth benefits for long-term declines in photosynthetic performance. We observed more rapid loss of PE-containing *T. amphioxeia* plastids in *H. pacifica*-fed *M. rubrum* populations than in starved populations, resulting in decreases in total plastid volume, cellular chlorophyll content, and photosynthetic capacity compared to starved cells. In part, changes in photophysiology may reflect lower per-chlorophyll photosynthetic performance in free-living *H. pacifica* than *T. amphioxeia* (Figure S5), but the ultimate impact is a reduction in cellular photosynthetic rates.

Although *M. rubrum*'s photosynthetic capacity is reduced by *H. pacifica* ingestion, over short time periods its growth accelerates with prey availability. Indeed, although saturating functions were the best statistical fits to our short-term (Experiment 1) data (Figure S3), our experiment did not include sufficiently high prey densities to directly measure saturated ingestion or growth rates (Figure 1). Rates of ingestion were more similar to, for example mixotrophic oligotrich ciliates (Gismervik, 2005; Schoener & McManus, 2017) than previous reports of *M. rubrum* (Johnson et al., 2006; Yih et al., 2004). It is possible that high rates of prey ingestion represent "luxury consumption" (Schoener & McManus, 2017) and allow *M. rubrum* to maintain fresh *H. pacifica* plastids. The gross growth efficiency (GGE; *M. rubrum* cells produced per *H. pacifica* cells ingested, Figure S9) indicated that about 27.5 *H. pacifica* cells would need to be ingested to produce one *M. rubrum* cell, which is much higher than observed ingestion rates for this species. (At low *H. pacifica* densities, legacy photosynthetic contributions of *T. amphioxeia* plastids appear to dominate the growth signal.) Using others' measurements of ~650 pg C per *M. rubrum* cell (Smith & Hansen, 2007; Stoecker et al., 1991) and our own prior measurements of ~40 pg C per *H. pacifica* (Moeller et al., 2021; Paight et al., 2023), we find that GGE_C ranges from 0.48 to 2.37 (Figure S10), which more closely resemble mixotrophic than phagotrophic ciliates (Hughes et al., 2021; Schoener & McManus, 2017). However, values less than 0.5 at high prey densities imply that *M. rubrum* growth could be substantially bolstered by heterotrophy when *H. pacifica* abundance is high.

Ultimately, the ingestion of *H. pacifica* plastids seemed to lead to a physiological "dead end" for

Eukaryotic Microbiology ISOP Published by the International Society of Protistologists

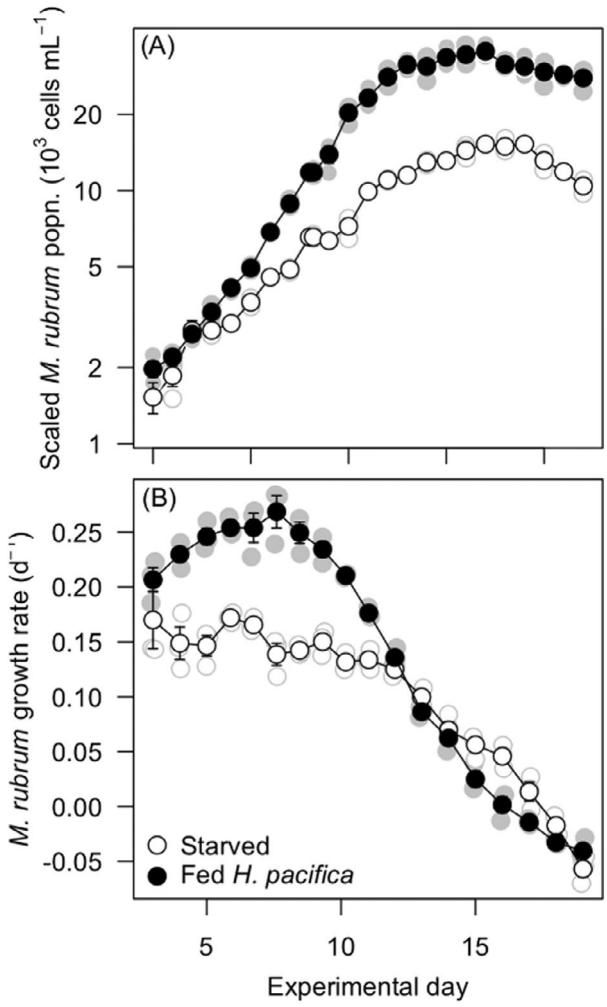

FIGURE 6 Long-term growth of *Mesodinium rubrum* is enhanced by the presence of *Hemiselmis pacifica*. (A) When fed *H. pacifica* (filled points), *M. rubrum* populations grew faster for a longer period of time, ultimately achieving larger population sizes over the 3-week experiment. (Note that *M. rubrum* population data have been rescaled to account for dilution; actual population sizes were below 10,000 cells/mL throughout the experiment.) (B) We used a sliding 7-day window to calculate growth rates, and found that feeding with *H. pacifica* increased *M. rubrum* growth rates for the first 12 days of the experiment, but in the final 10 days growth rates were similar between starved and fed treatments.

M. rubrum cells, whose accelerated growth halted after 2 weeks of experimental feeding. At this point, cell volumes also began to increase (Figure S6), and we saw numerous misshapen cells (personal observation; Figure S6). Together with microscopy observations that *H. pacifica* nuclei colocalize with *H. pacifica* plastids, and that ingested *H. pacifica* plastids are not arrayed along the outside of the cell like *T. amphioxeia* plastids, our findings suggest a breakdown in organelle handling, and perhaps cell division, with ingestion of alternative prey. In contrast, when fed *T. amphioxeia*, *M. rubrum* cell division is a synchronized and orderly event, with simultaneous division of plastids directed by the kleptokaryon, which is localized away from other prey organelles with the ciliate's own nuclei (Johnson et al., 2007, 2023; Johnson & Stoecker, 2005; Kim et al., 2017). Future research should explore cytoskeletal attachment of *H. pacifica*-containing vacuoles and their localization during ciliate mitosis.

Given long-term limitations to performance, why does *M. rubrum* ingest *H. pacifica*, especially when preferred prey are available? One reason may be that *H. pacifica* and *T. amphioxiea* are similar in cell size and swimming behavior (personal observation). Because *M. rubrum* is an ambush predator (Jiang & Johnson, 2021), similar motility patterns of the two cryptophytes may trigger the ciliate to capture and ingest them in the same way, in contrast to its ability to discriminate between, for example *T. amphioxeia* and *Storeatula major*, a substantially larger and slower swimming cryptophyte that tends to swim in short loops rather than long fast runs (Jiang & Johnson, 2021; Peltomaa & Johnson, 2017). Still, little is known about the physical and biochemical cues that mixoplankton like *M. rubrum* use to identify their prey.

Previous studies have also shown robust ingestion by *M. rubrum* of non-*Teleaulax* cryptophytes resulting in short-term positive growth, however, none have assessed how ingestion of alternate prey changes the photophysiology of *M. rubrum*. Hansen et al. (2012) found no evidence that organelles from nonpreferred cryptophytes were sequestered, and reported some ultrastructural changes to the thylakoid membrane of *Hemiselmis tepida* plastids that were interpreted as being consistent with exposure to digestive enzymes. Based on our observations of temporary retention of organelles with photosynthetically active plastids, it is unlikely that ingested *H. pacifica* prey are ingested specifically for heterotrophic digestion. However, they are clearly handled differently than ingested organelles from preferred *Teleaulax* prey, with the prey nucleus packaged along with the plastid and other organelles in a membrane and not moved to the cell perimeter. Superficially, this alternative prey organelle sequestration mechanism more closely resembles what is seen in *M. chamaeleon*, albeit with less stability of plastid function and longevity (Moeller et al., 2021). Collectively, these observations suggest that, when *M. rubrum* ingests nonpreferred cryptophyte prey, they fail to be sequestered, perhaps through some intracellular recognition process, and are instead retained until optimal prey is found. The fast replacement of these alternative prey organelles once the ciliate encounters *Teleaulax* suggests that optimal prey uptake may then stimulate quickened digestion or possibly egestion of these alternative prey organelles.

Ultimately, the presence of alternate prey may serve as an important, though time-limited ecological "bridge" for kleptoplastidic specialists like *M. rubrum* to tolerate low-resource environmental conditions until the presence of preferred prey can again support rapid growth (Herfort, Peterson, McCue, et al., 2011;

Johnson et al., 2016; Peterson et al., 2013). Indeed, we observed rapid replenishment of *T. amphioxeia* plastids and accelerated growth within 48 h of refeeding with preferred prey, consistent with other data showing rapid uptake of preferred organelles (Peterson et al., 2013). However, as its species name suggests, *M. rubrum* is not observed to have blue-green plastids in nature, suggesting that these interactions are relatively rare or transient. This may be due to different microhabitats used by *M. rubrum* and PC-containing *Hemiselmis* cryptophytes, or due to prey selectivity mechanisms that function in nature but not in the laboratory. Nevertheless, the ability to induce ingestion of alternate prey in laboratory settings opens new doors to exploring the cellular mechanisms of plastid integration via disruption with suboptimal prey.

AUTHOR CONTRIBUTIONS

HVM designed the research, carried out most experiments, performed analyses, and wrote the first draft of the article. AL-G designed, carried out, and analyzed data from the prey choice experiment. LV collected confocal microscopy data. AN developed FlowCam protocols, and GSB and AN collected preliminary data. GCR and JTK-R helped design the confocal data analysis pipeline. MDJ designed the research and advised on data analysis. All authors contributed to writing and revising the manuscript.

ACKNOWLEDGMENTS

We thank Felix Mikus for training on confocal image analysis tools and the Dey Lab at EMBL Heidelberg for feedback on the confocal-FlowCam calibration. We gratefully acknowledge funding from the US National Science Foundation Division of Molecular and Cellular Biosciences (MCB-2344640 to MDJ and MCB-2344641 to HVM), the Simons Foundation (Award 689265 to HVM), a University of California, Santa Barbara, Faculty Senate Research Grant (to HVM), and a visiting scholar grant from the Health + Life Science Alliance Heidelberg Mannheim (to HVM). We acknowledge NSF MRI grant DBI-1625770 and the UCSB NRI-MCDB Microscopy Facility for access to the Leica confocal microscope.

DATA AVAILABILITY STATEMENT

All data and codes used in this manuscript are available at https://doi.org/10.5281/zenodo.14201363.https://github.com/hollymoeller/MrubrumfedHpacifica

ORCID

Holly V. Moeller https://orcid.org/0000-0002-9335-0039
Matthew D. Johnson https://orcid.org/0000-0003-4853-2674

REFERENCES

Campbell, L., Olson, R.J., Sosik, H.M., Abraham, A., Henrichs, D.W., Hyatt, C.J. et al. (2010) First harmful *Dinophysis* (Dinophyceae, Dinophysiales) bloom in the U.S. is revealed by automated imaging flow cytometry. *Journal of Phycology*, 46, 66–75.

Cartaxana, P., Morelli, L., Quintaneiro, C., Calado, G., Calado, R. & Cruz, S. (2018) Kleptoplast photoacclimation state modulates the photobehaviour of the solar-powered sea slug *Elysia viridis*. *The Journal of Experimental Biology*, 221, jeb180463.

Ge, Y. & Sealfon, S.C. (2012) flowPeaks: a fast unsupervised clustering for flow cytometry data via K-means and density peak finding. *Bioinformatics*, 28, 2052–2058.

Gismervik, I. (2005) Numerical and functional responses of choreo- and oligotrich planktonic ciliates. *Aquatic Microbial Ecology*, 40, 163–173.

Gorbunov, M. & Falkowski, P.G. (2004) Fluorescence induction and relaxation (FIRe) technique and instrumentation for monitoring photosynthetic processes and primary production in aquatic ecosystems. In *Photosynthesis: Fundamental aspects to global perspectives* (pp. 1029–1031). Allen Press Montreal.

Guillard, R.R.L. & Ryther, J.H. (1962) Studies of marine planktonic diatoms: I. *Cyclotella nana* Hustedt, and *Detonula confervacea* (Cleve) gran. *Canadian Journal of Microbiology*, 8, 229–239.

Hansen, P.J., Moldrup, M., Tarangkoon, W., Garcia-Cuetos, L. & Moestrup, Ø. (2012) Direct evidence for symbiont sequestration in the marine red tide ciliate *Mesodinium rubrum*. *Aquatic Microbial Ecology*, 66, 63–75.

Hansen, P.J., Nielsen, L.T., Johnson, M., Berge, T. & Flynn, K.J. (2013) Acquired phototrophy in *Mesodinium* and *Dinophysis* – a review of cellular organization, prey selectivity, nutrient uptake and bioenergetics. *Harmful Algae*, 28, 126–139.

Hansen, P.J., Ojamäe, K., Berge, T., Trampe, E.C.L., Nielsen, L.T., Lips, I. et al. (2016) Photoregulation in a Kleptochloroplastidic dinoflagellate, *Dinophysis acuta*. *Frontiers in Microbiology*, 7, 785.

Hehenberger, E., Gast, R.J. & Keeling, P.J. (2019) A kleptoplastidic dinoflagellate and the tipping point between transient and fully integrated plastid endosymbiosis. *Proceedings of the National Academy of Sciences*, 116, 17934–17942.

Herfort, L., Peterson, T.D., Campbell, V., Futrell, S. & Zuber, P. (2011) Myrionecta rubra (*Mesodinium rubrum*) bloom initiation in the Columbia River estuary. *Estuarine, Coastal and Shelf Science*, 95, 440–446.

Herfort, L., Peterson, T.D., McCue, L.A., Crump, B.C., Prahl, F.G., Baptista, A.M. et al. (2011) *Myrionecta rubra* population genetic diversity and its cryptophyte chloroplast specificity in recurrent red tides in the Columbia River estuary. *Aquatic Microbial Ecology*, 62, 85–97.

Holling, C.S. (1959) Some characteristics of simple types of predation and parasitism. *Canadian Entomologist*, 91, 385–398.

Hughes, E.A., Maselli, M., Sørensen, H. & Hansen, P.J. (2021) Metabolic reliance on photosynthesis depends on both irradiance and prey availability in the mixotrophic ciliate, *Strombidium* cf. *Basimorphum*. *Frontiers in Microbiology*, 12, 642600.

Jeong, H.J. & Latz, M.I. (1994) Growth and grazing rates of the heterotrophic dinoflagellates *Protoperidinium* spp. on red tide dinoflagellates. *Marine Ecology Progress Series*, 106, 173–185.

Jiang, H. & Johnson, M.D. (2021) Swimming behavior of cryptophyte prey affects prey preference of the ambush-feeding ciliate *Mesodinium rubrum*. *Aquatic Microbial Ecology*, 86, 169–184.

Johnson, M.D. (2011) The acquisition of phototrophy: adaptive strategies of hosting endosymbionts and organelles. *Photosynthesis Research*, 107, 117–132.

Johnson, M.D., Beaudoin, D.J., Frada, M.J., Brownlee, E.F. & Stoecker, D.K. (2018) High grazing rates on Cryptophyte algae in Chesapeake Bay. *Frontiers in Marine Science*, 5, 241.

Johnson, M.D., Beaudoin, D.J., Laza-Martinez, A., Dyhrman, S.T., Fensin, E., Lin, S. et al. (2016) The genetic diversity of *Mesodinium* and associated cryptophytes. *Frontiers in Microbiology*, 7, 2017.

Johnson, M.D., Moeller, H.V., Paight, C., Kellogg, R.M., McIlvin, M.R., Saito, M.A. et al. (2023) Functional control and metabolic

integration of stolen organelles in a photosynthetic ciliate. *Current Biology*, 33, 973–980.e5.

Johnson, M.D., Oldach, D., Delwiche, C.F. & Stoecker, D.K. (2007) Retention of transcriptionally active cryptophyte nuclei by the ciliate *Myrionecta rubra*. *Nature*, 445, 426–428.

Johnson, M.D. & Stoecker, D.K. (2005) Role of feeding in growth and photophysiology of *Myrionecta rubra*. *Aquatic Microbial Ecology*, 39, 303–312.

Johnson, M.D., Tengs, T., Oldach, D. & Stoecker, D.K. (2006) Sequestration, performance, and functional control of cryptophyte plastids in the ciliate *Myrionecta rubra* (Ciliophora). *Journal of Phycology*, 42, 1235–1246.

Karnkowska, A., Yubuki, N., Maruyama, M., Yamaguchi, A., Kashiyama, Y., Suzaki, T. et al. (2023) Euglenozoan kleptoplasty illuminates the early evolution of photoendosymbiosis. *Proceedings of the National Academy of Sciences*, 120, e2220100120.

Kim, M., Drumm, K., Daugbjerg, N. & Hansen, P.J. (2017) Dynamics of sequestered cryptophyte nuclei in *Mesodinium rubrum* during starvation and refeeding. *Frontiers in Microbiology*, 8, 423.

Kim, M., Kang, M. & Park, M.G. (2019) Growth and chloroplast replacement of the benthic mixotrophic ciliate *Mesodinium coatsi*. *The Journal of Eukaryotic Microbiology*, 66, 625–636.

Lepori-Bui, M., Paight, C., Eberhard, E., Mertz, C.M. & Moeller, H.V. (2022) Evidence for evolutionary adaptation of mixotrophic nanoflagellates to warmer temperatures. *Global Change Biology*, 28, 7094–7107.

Miyagishima, S. (2023) Taming the perils of photosynthesis by eukaryotes: constraints on endosymbiotic evolution in aquatic ecosystems. *Communications Biology*, 6, 1–15.

Moeller, H.V., Hsu, V., Lepori-Bui, M., Mesrop, L.Y., Chinn, C. & Johnson, M.D. (2021) Prey type constrains growth and photosynthetic capacity of the kleptoplastidic ciliate *Mesodinium chamaeleon* (Ciliophora). *Journal of Phycology*, 57, 916–930.

Moeller, H.V. & Johnson, M.D. (2018) Preferential plastid retention by the acquired phototroph *Mesodinium chamaeleon*. *The Journal of Eukaryotic Microbiology*, 65, 148–158.

Moeller, H.V., Peltomaa, E., Johnson, M.D. & Neubert, M.G. (2016) Acquired phototrophy stabilises coexistence and shapes intrinsic dynamics of an intraguild predator and its prey. *Ecology Letters*, 19, 393–402.

Moestrup, Ø., Garcia-Cuetos, L., Hansen, P.J. & Fenchel, T. (2012) Studies on the genus *Mesodinium* I: ultrastructure and description of *Mesodinium chamaeleon* n. sp., a benthic marine species with green or red chloroplasts. *The Journal of Eukaryotic Microbiology*, 59, 20–39.

Monod, J. (1949) The growth of bacterial cultures. *Annual Review of Microbiology*, 3, 371–394.

Montagnes, D.J.S., Allen, J., Brown, L., Bulit, C., Davidson, R., Díaz-Ávalos, C. et al. (2008) Factors controlling the abundance and size distribution of the phototrophic ciliate *Myrionecta rubra* in open waters of the North Atlantic. *The Journal of Eukaryotic Microbiology*, 55, 457–465.

Myung, G., Kim, H.S., Park, J.S., Park, M.G. & Yih, W. (2011) Population growth and plastid type of *Myrionecta rubra* depend on the kinds of available cryptomonad prey. *Harmful Algae*, 10, 536–541.

Myung, G., Yih, W., Kim, H.S., Park, J.S. & Cho, B.C. (2006) Ingestion of bacterial cells by the marine photosynthetic ciliate *Myrionecta rubra*. *Aquatic Microbial Ecology*, 44, 175–180.

Paight, C., Johnson, M.D., Lasek-Nesselquist, E. & Moeller, H.V. (2023) Cascading effects of prey identity on gene expression in a kleptoplastidic ciliate. *The Journal of Eukaryotic Microbiology*, 70, e12940.

Park, J.S., Myung, G., Kim, H.S., Cho, B.C. & Yih, W. (2007) Growth responses of the marine photosynthetic ciliate *Myrionecta rubra* to different cryptomonad strains. *Aquatic Microbial Ecology*, 48, 83–90.

Peltomaa, E. & Johnson, M.D. (2017) *Mesodinium rubrum* exhibits genus-level but not species-level cryptophyte prey selection. *Aquatic Microbial Ecology*, 78, 147–159.

Peterson, T.D., Golda, R.L., Garcia, M.L., Li, B., Maier, M.A., Needoba, J.A. et al. (2013) Associations between *Mesodinium rubrum* and cryptophyte algae in the Columbia River estuary. *Aquatic Microbial Ecology*, 68, 117–130.

R Core Team. (2023) R: A language and environment for statistical computing. Available from: https://www.R-project.org/

Schindelin, J., Arganda-Carreras, I., Frise, E., Kaynig, V., Longair, M., Pietzsch, T. et al. (2012) Fiji: an open-source platform for biological-image analysis. *Nature Methods*, 9, 676–682.

Schoener, D.M. & McManus, G.B. (2017) Growth, grazing, and inorganic C and N uptake in a mixotrophic and a heterotrophic ciliate. *Journal of Plankton Research*, 39, 379–391.

Smith, M. & Hansen, P.J. (2007) Interaction between *Mesodinium rubrum* and its prey: importance of prey concentration, irradiance and pH. *Marine Ecology Progress Series*, 338, 61–70.

Speijer, D., Hammond, M. & Lukeš, J. (2020) Comparing early eukaryotic integration of mitochondria and chloroplasts in the light of internal ROS challenges: timing is of the essence. *MBio*, 11. Available from: https://doi.org/10.1128/mbio.00955-20

Stoecker, D.K., Johnson, M.D., Vargas, C.d. & Not, F. (2009) Acquired phototrophy in aquatic protists. *Aquatic Microbial Ecology*, 57, 279–310.

Stoecker, D.K., Putt, M., Davis, L.H. & Michaels, A.E. (1991) Photosynthesis in Mesodinium rubrum: species-specific measurements and comparison to community rates. *Marine Ecology Progress Series*, 73, 245–252.

Wisecaver, J.H. & Hackett, J.D. (2010) Transcriptome analysis reveals nuclear-encoded proteins for the maintenance of temporary plastids in the dinoflagellate *Dinophysis acuminata*. *BMC Genomics*, 11, 366.

Yamada, N., Lepetit, B., Mann, D.G., Sprecher, B.N., Buck, J.M., Bergmann, P. et al. (2023) Prey preference in a kleptoplastic dinoflagellate is linked to photosynthetic performance. *The ISME Journal*, 17, 1578–1588.

Yih, W., Kim, H.S., Jeong, H.J., Myung, G. & Kim, Y.G. (2004) Ingestion of cryptophyte cells by the marine photosynthetic ciliate *Mesodinium rubrum*. *Aquatic Microbial Ecology*, 36, 165–170.

SUPPORTING INFORMATION

Additional supporting information can be found online in the Supporting Information section at the end of this article.

How to cite this article: Moeller, H.V., L'Etoile-Goga, A., Vincenzi, L., Norlin, A., Barbaglia, G.S., Runte, G.C. et al. (2025) Retention of blue-green cryptophyte organelles by *Mesodinium rubrum* and their effects on photophysiology and growth. *Journal of Eukaryotic Microbiology*, 72, e13066. Available from: https://doi.org/10.1111/jeu.13066